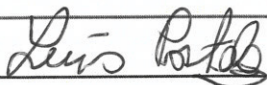


GRANT AGREEMENT No.: 764902 Project Acronym: TOMOCON Project title: Smart tomographic sensors for advanced industrial process control			
Deliverable Rel. No. D5.2.		Lead Beneficiary TUD	
EU Del. No. D16		Type Report	
WP No. WP5		Date: 29.10.2019	Revision: 0
Innovative Training Network TOMOCON			
Deliverable Title <h2 style="text-align: center;">Detailed Plan for Lab Demonstrations</h2>			
Description <p>This deliverable describes the lab-scale demonstrations including the facility descriptions, process conditions, used experimental techniques, goals and objectives as well as the mode and timeline of execution.</p>			

Prepared by:	Dr. Luis Portela	
Approved by:	Prof. Dr. Uwe Hampel	
Approved by Supervisory Board:	30.10.2019	

Dissemination Level: **Public**



This project has received funding from the European Union's Horizon 2020 research and innovation programme under the Marie Skłodowska-Curie Grant Agreement No. 764902.

TOMOCON			GRANT AGREEMENT No.: 764902		
Deliverable Title: Detailed Plan for Lab Demonstrations					
Del. Rel. No.	EU Del. No.	WP No.	Lead Beneficiary	Type	Date
D5.2.	D16	WP5	TUD	Report	29.10.2019

Revision Sheet

Revision Number	Purpose of Revision	Effective Date
0	Initial Issue	30.10.2019



TOMOCON			GRANT AGREEMENT No.: 764902		
Deliverable Title: Detailed Plan for Lab Demonstrations					
Del. Rel. No.	EU Del. No.	WP No.	Lead Beneficiary	Type	Date
D5.2.	D16	WP5	TUD	Report	29.10.2019

Table of Contents

Detailed Plan for Lab Demonstrations	5
1. Inline Fluid Separation	5
1.1. Experimental apparatus	5
1.2. Explored conditions	6
1.3. Used experimental techniques	7
1.4. Goals and objectives	8
1.4.1. Goals	8
1.4.2. Objectives	9
1.5. Mode and timeline of execution	9
1.6. References	10
2. Microwave Drying	11
2.1. Facility description	11
2.2. Process conditions	11
2.3. Used experimental techniques	12
2.3.1. Electrical Capacitance Tomography (ECT) sensor	13
2.3.2. Microwave Tomography (MWT) sensor	14
2.3.3. Interactive visualization of process data	14
2.4. Goals and objectives	15
2.5. Mode and timeline of execution	16
3. Continuous Casting	17
3.1. Facility description	17
3.2. Process conditions	19
3.3. Used experimental techniques	20
3.3.1. Contactless inductive flow tomography (CIFT)	20
3.3.2. Combined MIT and ECT	21
3.3.3. Ultrasound Doppler Velocimetry (UDV)	22
3.4. Goals and objectives	22
3.5. Mode and timeline of execution	24
4. Batch Crystallization	25
4.1. Facility description	25



TOMOCON			GRANT AGREEMENT No.: 764902		
Deliverable Title: Detailed Plan for Lab Demonstrations					
Del. Rel. No.	EU Del. No.	WP No.	Lead Beneficiary	Type	Date
D5.2.	D16	WP5	TUD	Report	29.10.2019

4.2.	Process conditions.....	27
4.3.	Used experimental techniques.....	28
4.4.	Goals and objectives	29
4.5.	Mode and timeline of execution	30
4.6.	References	31



TOMOCON			GRANT AGREEMENT No.: 764902		
Deliverable Title: Detailed Plan for Lab Demonstrations					
Del. Rel. No.	EU Del. No.	WP No.	Lead Beneficiary	Type	Date
D5.2.	D16	WP5	TUD	Report	29.10.2019

Detailed Plan for Lab Demonstrations

1. Inline Fluid Separation

1.1. Experimental apparatus

The inline fluid separation demonstration will be performed at TU Delft. The flow loop was designed at the university and the main flow takes place inside an 81.4 mm I.D. (90 mm O.D.) vertical pipe with around 6 m length.

The injection of air in the loop takes place at 4 m (50D) before the swirl element. The condition ensures a reasonable development length for the multiphase flow before it reaches the swirling region thereby minimizing the dependency of the results on the injection method.

To create the swirl flow, the swirl elements of a previous setup (van Campen, 2014) [1] were adopted. They were designed for a 100 mm diameter pipe. The flow is therefore expanded right before the element and contracted right after it. A picture of the swirl elements designed in this previous work is shown in Figure 1.

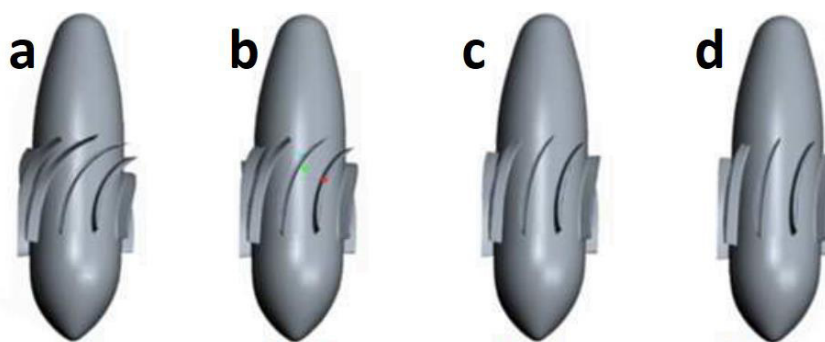


Figure 1: Swirl elements designed by van Campen (2014) [1]. Figure obtained from Star (2016) [2].
a) Vane angle of 73° in relation to a vertical line **b)** Vane angle of 63.1° **c)** Vane angle of 51.5°
d) Vane angle of 40.2°

The swirl elements of Figure 1 present different vane angles, thus generating different intensities of swirl motion. The flow conditions must still be tested, but the idea is to proceed with the swirl element that generates the smallest swirl motion but still creates a gas core. The condition is especially important to approximate the flow to the real oil-water application of such separators where an oversized swirl motion impacts the efficiency of separation and may lead to emulsions. To achieve such a goal, the weaker swirl element is probably going to be used in the final demonstration. This element presents a blade angle of 51.5° , and creates an azimuthal velocity of 3 times the bulk one at the inlet of the swirl pipe.

TOMOCON				GRANT AGREEMENT No.: 764902	
Deliverable Title: Detailed Plan for Lab Demonstrations					
Del. Rel. No.	EU Del. No.	WP No.	Lead Beneficiary	Type	Date
D5.2.	D16	WP5	TUD	Report	29.10.2019

A swirl tube of 15D is going to be used in the demonstration and a pickup tube of 40 mm external diameter is initially considered to capture the gas core formed inside the separator. The separation is controlled by two valves, placed individually in each one of the outlets of the separator (light and heavy phase outlets). A schematics of the separator is shown in Figure 2.

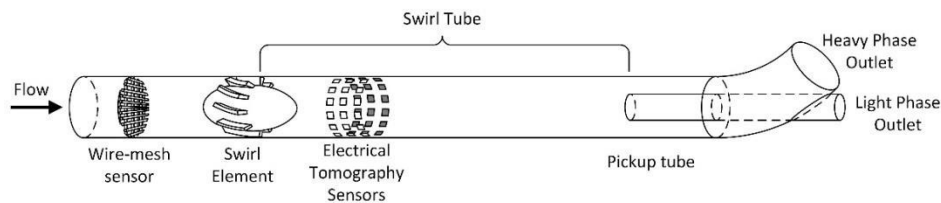


Figure 2: Schematics of the separator used in the project

The wire-mesh sensor is used to measure the distribution of the gas and liquid phases before the swirl element, then characterizing the inlet conditions. The Electrical Resistance Tomography sensor is placed inside the swirl pipe and is used to measure the core of gas generated by the swirl motion. Both sensors are used in combination in the control step.

1.2. Explored conditions

The flow rates considered for the demonstration are based on the bubbly flow pattern happening before the swirl element. The exploration of part of the region containing the churn / slug patterns is also desired, but its appearance in the demonstration depends on the success of the approach currently under development as well as on the ability of the sensors to handle high flow rates that result in smaller timescales of the flow.

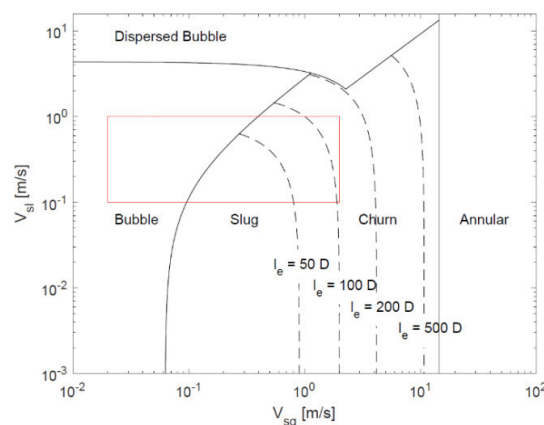


Figure 3: Flow rates explored in the setup. Patterns obtained according to Taitel et al. (1980) [3].

TOMOCON				GRANT AGREEMENT No.: 764902	
Deliverable Title: Detailed Plan for Lab Demonstrations					
Del. Rel. No.	EU Del. No.	WP No.	Lead Beneficiary	Type	Date
D5.2.	D16	WP5	TUD	Report	29.10.2019

The exact conditions explored in the final demonstration still have to be decided. The flow loop is designed to handle the inlet conditions inside the red square of Figure 3. For the final demonstration, two or three points inside the bubbly flow region contained by the square are going to be explored.

To be considered successfully, the approach must result in a considerable increase in efficiency in relation to the uncontrolled separator. Both conditions are going to be presented in the final demonstration.

A dispersed efficiency is considered to quantitatively judge the flow. Its value is 100 % only if all the water leaves the pipe through the water outlet and, simultaneously, all the air is captured by the pickup tube. The gain in the efficiency of the equipment will be displayed in the final results.

The transparent characteristic of the pipe in the location of the separation and its accessibility also allow an intuitive and very visual checking of the performance of the control strategy. Pictures of the location for different conditions of operation may be included in the final report.

The opening of the valves placed at the outlets of the separator are the only variables used during the control step. Multiple valves can be used at the location to achieve a faster response. In case the valves are not sufficient to control the flow, controllable blades are going to be installed in the swirl element. However, the approach is highly undesirable, due to the mechanical complexity introduced in the device, which is not desired in real applications.

1.3. Used experimental techniques

The wire-mesh sensor is used to obtain the flow characteristics before the separation, while the electrical tomography sensor is used to measure the behaviour of the flow inside it. Both sensors are used in combination in the control step. Ideally, the wire-mesh sensor will be used to speed up the tomographic sensor downstream the swirl element, allowing it to increase its performance. However, the procedure is still conceptual at this point.

Additional (common) sensors are considered in the measurements, as flow meters and pressure gauges. Their use in the control loop still has to be determined within the next months. However, it is worth mentioning that these sensors are going to be employed only, if they are really required; there is an interest in restraining the number of sensors to the ones developed inside the group.

The proposed control loop is shown in Figure 4. The core radius (or area) is considered in the control approach and a MPC controller is used to set the valves that best approach the core size at the pickup tube location to the pickup tube diameter itself (thus maximizing the efficiency of separation). It must be noted that, as the strategy is to capture the entire gas core, the predicted gas core diameter expected change is limited to the pickup tube diameter.



TOMOCON			GRANT AGREEMENT No.: 764902		
Deliverable Title: Detailed Plan for Lab Demonstrations					
Del. Rel. No.	EU Del. No.	WP No.	Lead Beneficiary	Type	Date
D5.2.	D16	WP5	TUD	Report	29.10.2019

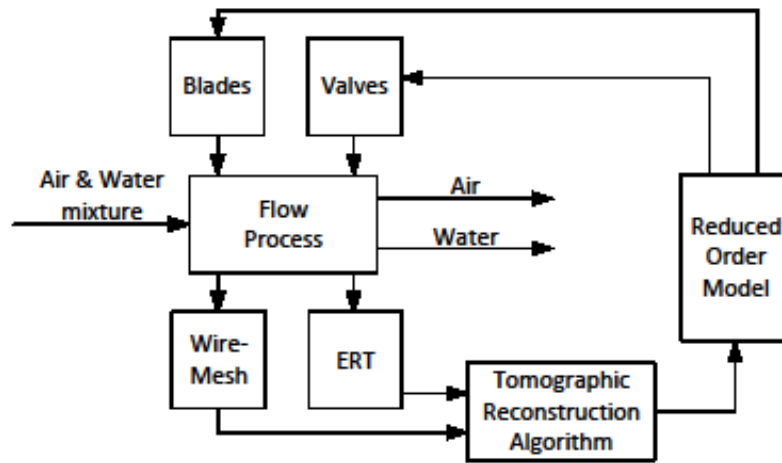


Figure 4: Proposed control strategy

Due to the low residence time of the flow inside the separator, high fps cameras can be used as support to facilitate the visualization of the separation in the final demonstration, as previously mentioned. These cameras are also going to be used during the experiments before the final demonstration, as they allow the visualization of a cross-section of the flow perpendicular to the tomographic sensors, complementing their measurements and allowing an understanding of the physics happening inside the device.

1.4. Goals and objectives

1.4.1. Goals

Regarding the sensors, a high frequency of acquisition is expected. They should be able to measure the flow fast enough to ensure the stability of the control loop, i.e. they cannot be the bottleneck of the controlled device. Their spatial resolution is a secondary priority; the gas core has to be tracked over time but minor structures as dispersed bubbles are not that important as they contribute much less to the efficiency of separation in an air-water flow. The use of Graphic Processing Units is being studied to speed up the reconstruction step of such devices.

The control plant, i.e. the reduced order model connecting the transient gas core behavior with the action of the valves, has to be fast enough to be computed in real time.

The MPC controller should be able to control the flow. It has to consider in its design (i) the time response of the valves, (ii) the time resolution of the sensors and (iii) the time involved in computing the best output for the valves.

The set of valves at the outlets should be quick enough to affect the flow. This may require creative solutions on how to employ them, as the use of multiple elements.



TOMOCON				GRANT AGREEMENT No.: 764902		
Deliverable Title: Detailed Plan for Lab Demonstrations						
Del. Rel. No.	EU Del. No.	WP No.	Lead Beneficiary	Type	Date	
D5.2.	D16	WP5	TUD	Report	29.10.2019	

1.4.2. Objectives

An increase of the separation efficiency is the final objective of the project. The performance of the device is going to be judged according to (i) its ability of capturing the whole gas phase present in the flow, (ii) its ability of achieving such a goal while capturing the least possible amount of water and (iii) the time required to reach this condition with a change in the inlet of the flow.

1.5. Mode and timeline of execution

Topic	Task	Responsible	2019		2020									
			Nov	Dec	Jan	Feb	Mar	April	May	Jun	Jul	Aug	Sep	
WMS	Ensure that the wire-mesh sensor is able to operate at a frequency of 1000 Hz	Ben + HZDR (ESR 1)	█											
	Fabrication of a sensor that fits the final loop; hardware and software parts		█	█	█	█				█	█	█		
	Installation and adaptation of this sensor in the loop													█
ERT	Study different strategies of maximizing the sensor acquisition rate	Muhammad (ESR 10)	█	█	█	█	█							
	Study the use of an external input in the sensor, to speed up the tomographic reconstruction		█	█										
	Fabrication of a sensor that fits the final loop									█	█	█		
	Installation and adaptation of this sensor in the loop													█
ROM	Development of a reduced order model representative of the flow	Matheus (ESR 4)	█			█	█	█						
	Validation of this model with experiments and CFD simulations	Matheus (ESR 4) Hanane (ESR 6)												
	Adjustments in the model	Matheus (ESR 4)												
MPC	Initial (virtual) implementation of a MPC controller	Matheus (ESR 4) + TU Delft Technicians				█	█	█						
	Adjustment of the weight functions based on goals/response of the virtual tests												█	
	Virtual validation of the controller									█	█			
	Implementation in the real flow loop												█	
Flow loop	Building it		█	█	█									
	Measurements and tests												█	
	Adjustments to final demonstration												█	



TOMOCON			GRANT AGREEMENT No.: 764902		
Deliverable Title: Detailed Plan for Lab Demonstrations					
Del. Rel. No.	EU Del. No.	WP No.	Lead Beneficiary	Type	Date
D5.2.	D16	WP5	TUD	Report	29.10.2019

1.6. References

- [1] L. van Campen, Bulk Dynamics of Droplets in Liquid-Liquid Axial Cyclones, PhD Thesis, Delft University of Technology, 2014.
- [2] S. K. Star, Pressure distribution in a liquid-liquid cyclone separator, Master Thesis, Delft University of Technology, 2016.
- [3] Y. Taitel, D. Bornea, A. E. Dukler, Modelling Flow Pattern Transitions for Steady Upward Gas-Liquid Flow in Vertical Tubes, AIChE Journal, 1980.



TOMOCON			GRANT AGREEMENT No.: 764902		
Deliverable Title: Detailed Plan for Lab Demonstrations					
Del. Rel. No.	EU Del. No.	WP No.	Lead Beneficiary	Type	Date
D5.2.	D16	WP5	TUD	Report	29.10.2019

2. Microwave Drying

2.1. Facility description

The demonstration of a microwave drying process with support of ECT and MWT for improved process control will be performed on an industrial scale conveyor belt system that allows heating with microwave in combination with convective heating. That system was developed within a joint public funded R&D national project with the industrial partner Vötsch Industrietechnik, also partner in the TOMOCON Consortium. It comprises an applicator 4 m in length with 36 kW installed microwave power on 18 individual slotted waveguide antennas and 28 kW of convective heating power. On both ends the system uses an input and output tunnel of 1.5 m in length that allows the installation of filters and absorbers to reduce potential microwave leakage.

Such filter designs need to be adapted to any change in shape and dielectric properties of processed materials to guarantee maximum suppression of the microwave leakage. Since this is not part of the project, within the TOMOCON project we have to rely on a water based microwave absorber only. Even in case the leakage could be successfully suppressed below the permitted power level of 5 mW/cm², the power levels might still be too high and may influence the highly sensitive MWT signals. Therefore, the novel MWT design needs to take care about that issue.



Figure 5: Photo of the industrial scale microwave system at KIT that will be used for the drying of porous foam in a continuous process

2.2. Process conditions

This conveyor belt industrial microwave system will be used to demonstrate a microwave drying process of porous foams provided by the TOMOCON industrial partner Pinta. A continuous foam with 0.5 m in width, up to 7.5 cm in height and infinite length will be conveyed



TOMOCON			GRANT AGREEMENT No.: 764902		
Deliverable Title: Detailed Plan for Lab Demonstrations					
Del. Rel. No.	EU Del. No.	WP No.	Lead Beneficiary	Type	Date
D5.2.	D16	WP5	TUD	Report	29.10.2019

through the microwave system for fast and energy efficient drying. The moisture content of the impregnated and wet foam before entering the microwave system is in the range of about 50 weight% on the basis of the wet foam.

To be qualified for the final application, the target moisture content of the processed and dry materials, according to the information of Pinta, should be below 15 wt.% on wet basis in any part of the processed foam.

To achieve this moisture level the following process parameters are controllable:

- Conveyor belt speed
- Average microwave power level
- Microwave power level on each of the 18 individual antennas
- Convective air temperature
- Convective air speed



Figure 6: Photo of the industrial scale microwave system at KIT during operation with a continuous polymer foam from Pinta

2.3. Used experimental techniques

For better process control and / or validation of the dry state of the foam, an ECT and / or MWT sensor will be installed behind the output port of the conveyor belt system. This will allow in-situ measurement of moisture distribution and moisture level. The information of that will be fed into the intelligent control algorithm to control the parameters given in section 2.2.



TOMOCON				GRANT AGREEMENT No.: 764902		
Deliverable Title: Detailed Plan for Lab Demonstrations						
Del. Rel. No.	EU Del. No.	WP No.	Lead Beneficiary	Type	Date	
D5.2.	D16	WP5	TUD	Report	29.10.2019	

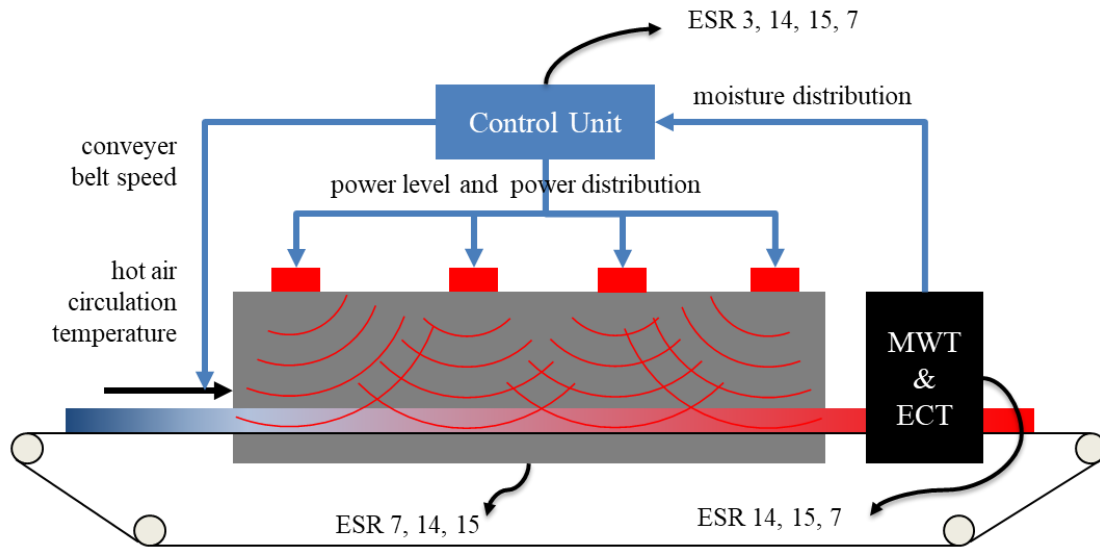


Figure 7: Scheme of the microwave system with information about potential control parameters and ESR responsibilities

2.3.1. Electrical Capacitance Tomography (ECT) sensor

One of the tomographic sensors used is the ECT sensor which consists of several electrodes mounted around the target. By applying electrical voltage to one of the electrodes, the electrical capacitances between the other electrodes can be measured. By repeating this measurement procedure by having each of the electrodes as a source, the electrical permittivity of the target can be reconstructed. Fig. 8 shows the designed and built ECT sensor for this demonstration using 12 electrodes on the top and bottom surfaces. MATLAB and NetGen software are used to design the sensor geometry and create its mesh. The time resolution of the ECT system is around 25 Hz.

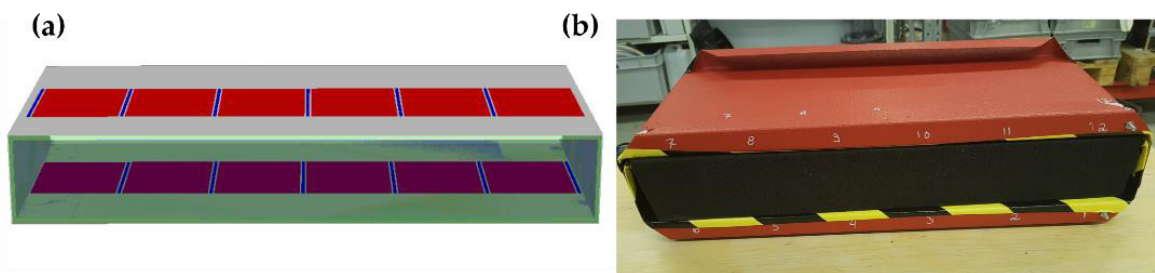


Figure 8: ECT sensor prototype (a) NetGen design (b) The built sensor while measuring the permittivity of an impregnated foam sample

TOMOCON			GRANT AGREEMENT No.: 764902		
Deliverable Title: Detailed Plan for Lab Demonstrations					
Del. Rel. No.	EU Del. No.	WP No.	Lead Beneficiary	Type	Date
D5.2.	D16	WP5	TUD	Report	29.10.2019

2.3.2. Microwave Tomography (MWT) sensor

The second sensor technique to be developed and demonstrated is a microwave tomography (MWT) sensor. It is used as an imaging modality to reconstruct the moisture content distribution in a porous foam during its microwave drying process.

MWT is a technique of estimating the material properties (dielectric constant, conductivity) of an object from the measured data of a scattered electromagnetic field. An antenna array system is used to measure the scattered electric field in terms of S-parameter. The MWT setup used for the virtual demonstration of the present work is shown in Fig. 9.

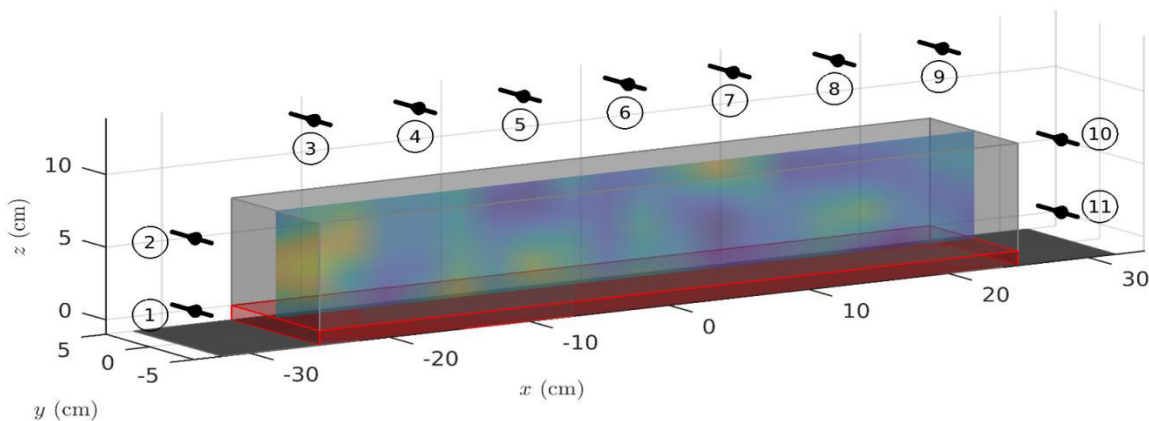


Figure 9: Model used for benchmarking purposes. The light gray box is the porous foam and the red box the conveyor belt while the dark gray surface denotes the perfect electric conductor (PEC) boundary. The antenna array is visualized with black cylinders and the color surface inside the porous foam illustrates the potential moisture density field on the cross section where $y=0$ cm.

In order to develop a microwave tomography (MWT) system, which is capable to extract the moisture distribution and moisture level inside the foam and distinguish between different moisture levels, the proper operation frequency should be obtained as the first step. Based on this operation frequency, a suitable Horn antenna will be employed (chosen due to overcoming the high power interference) to the transmitting / receiving signal into the medium.

2.3.3. Interactive visualization of process data

Instruments that allow operators to communicate and interact with the process will support the process control. For process condition monitoring, there are some infrared cameras mounted on the top surface of the chamber which are used to record the whole drying process. After capturing a large amount of infrared images (see Fig. 10) frame by frame from infrared videos, we are eligible to do condition monitoring using deep learning via those images. The areas of high moisture, low moisture could be detected precisely as well as the fault area if existing.

TOMOCON			GRANT AGREEMENT No.: 764902		
Deliverable Title: Detailed Plan for Lab Demonstrations					
Del. Rel. No.	EU Del. No.	WP No.	Lead Beneficiary	Type	Date
D5.2.	D16	WP5	TUD	Report	29.10.2019

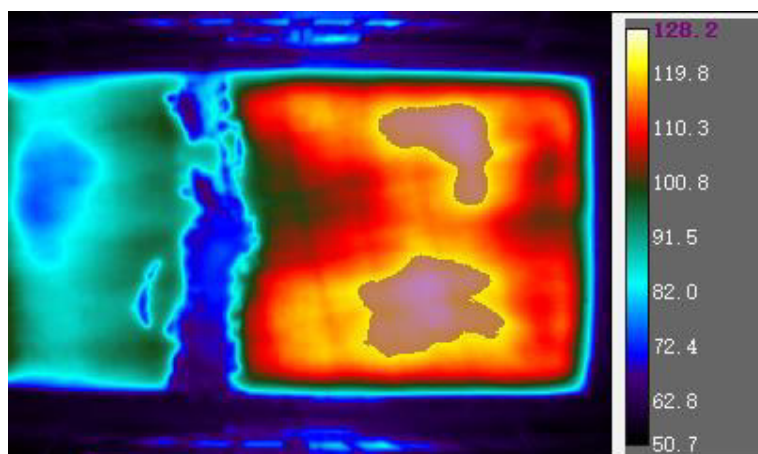


Figure 10: Example of infrared image

2.4. Goals and objectives

The goals and objectives in the demonstration part of microwave drying are first of all the design and development of appropriate ECT and MWT sensors that fit to the targeted process conditions. The tomographic sensors should provide a resolution in space and moisture level to provide reasonable information that is valuable for the process control. The special resolution should be in the range of half wavelength of the operation frequency of the microwave system and the resolution for moisture level measurements should be ± 2 weight% of the wet basis at a level of 15 weight%.

ECT and MWT sensors need to be adapted to and installed in the existing industrial scale microwave system described in section 2.1. The already well-trained inverse problem solver of the ECT and MWT shall provide appropriate information that will allow the controller to set the appropriate process parameters listed in section 2.2.

To do so the controller software needs to be transferred into a code that allows communication with the Simpac software from Vötsch. In case this is not feasible, a completely new software independent from Simpac needs to be developed which might need significantly more efforts. Furthermore, an in-situ visualization of the process parameters and moisture distribution will be implemented and will support system operators and process control.

As soon as everything has been implemented, the microwave drying process will be demonstrated and achieved benefits for the process will have to be evaluated. The benchmark target is a reduction of the drying time of up to 25 % and a quantification of the associated energy savings.



TOMOCON				GRANT AGREEMENT No.: 764902		
Deliverable Title: Detailed Plan for Lab Demonstrations						
Del. Rel. No.	EU Del. No.	WP No.	Lead Beneficiary	Type	Date	
D5.2.	D16	WP5	TUD	Report	29.10.2019	

2.5. Mode and timeline of execution

Task	Responsible ESR	2019												2020						
		Year												Year						
		Month	Jun	Jul	Aug	Sep	Oct	Nov	Dec	Jan	Feb	Mar	Apr	May	Jun	Jul	Aug	Sep	Oct	Nov
ECT																				
Design adapted to demonstration needs	ESR 14																			
Fabrication of ECT for demonstration	ESR 14																			
MW system modified and ECT installed	ESR 7, 14																			
ECT tested during MW system operation	ESR 7, 14																			
MWT																				
Design adapted to demonstration needs	ESR 7																			
Fabrication of MWT for demonstration	ESR 7																			
MW system modified and MWT installed	ESR 7																			
MWT tested during MW system operation	ESR 7, 15																			
Control																				
Control algorithms development and testing in virtual demonstration	ESR 3, 14																			
Implementation of control algorithm in Vötsch industrial control software	ESR 3, 7, 14																			
Installation and testing of hardware for foam impredation and heating	ESR 7																			
Demonstration																				
ECT																				
Installation of ECT	ESR 3, 7, 14, 15																			
Final tests on minor software correction before demonstration	ESR 3, 7, 14, 15																			
Demo of MW drying with full operation of ECT and improve control	ESR 3, 7, 14, 15																			
MWT																				
Installation of MWT	ESR 3, 7, 14, 15																			
Final tests on minor software correction before demonstration	ESR 3, 7, 14, 15																			
Demo of MW drying with full operation of ECT and improve control	ESR 3, 7, 14, 15																			



TOMOCON			GRANT AGREEMENT No.: 764902		
Deliverable Title: Detailed Plan for Lab Demonstrations					
Del. Rel. No.	EU Del. No.	WP No.	Lead Beneficiary	Type	Date
D5.2.	D16	WP5	TUD	Report	29.10.2019

3. Continuous Casting

3.1. Facility description

The demonstrator of continuous casting will be a small scale model of a continuous caster. Schematics and a picture of the Mini-LIMMCAST facility are shown in Figure 11. It is operated with the eutectic alloy of Gallium-Indium-Tin (GaInSn) which is liquid at room temperature. The liquid metal is stored in the catchment tank, from where it is pumped to the tundish using a MHD pump. The level of the liquid metal in the tundish is continuously kept constant by controlling the speed of the pump. From the tundish the metal flows through the submerged entry nozzle (SEN) to the mould, and the flow rate is set by opening (lifting) or closing (lowering) the stopper rod. The continuous loop operation of the facility ensures a well-developed flow in the mould, and a long runtime of experiments. Additionally, Mini-LIMMCAST has the possibility to be equipped with additional actuating equipment, such as an electromagnetic brake (EMBr), an electromagnetic stirrer (EMS), and a gas flow injector and regulator.

For the demonstrator in the TOMOCON project, a mould with a rectangular cross section of 300 mm x 35 mm with a height of 670 mm was built, which is made out of PPMA. A schematic is shown in Figure 12. The used electromagnetic brake is shown in detail in Figure 13. The EMBr generates a strong static magnetic field perpendicular to the wide faces of the mould. If the liquid metal flows through this magnetic field, electrical currents are induced in the liquid, which generates in combination with the static magnetic field a Lorentz force in the fluid. This force is used to control the flow condition in the mould. The EMBr is powered by two Heinzinger Electronic current sources connected in parallel and controlled from the PC via a RS232 port. At a maximum current of 600 A, the EMBr generates a magnetic flux density of 404 mT. The EMBr is water cooled, allowing for an operation for several hours with maximum current. The current and the temperature of the brake are measured during the operation.

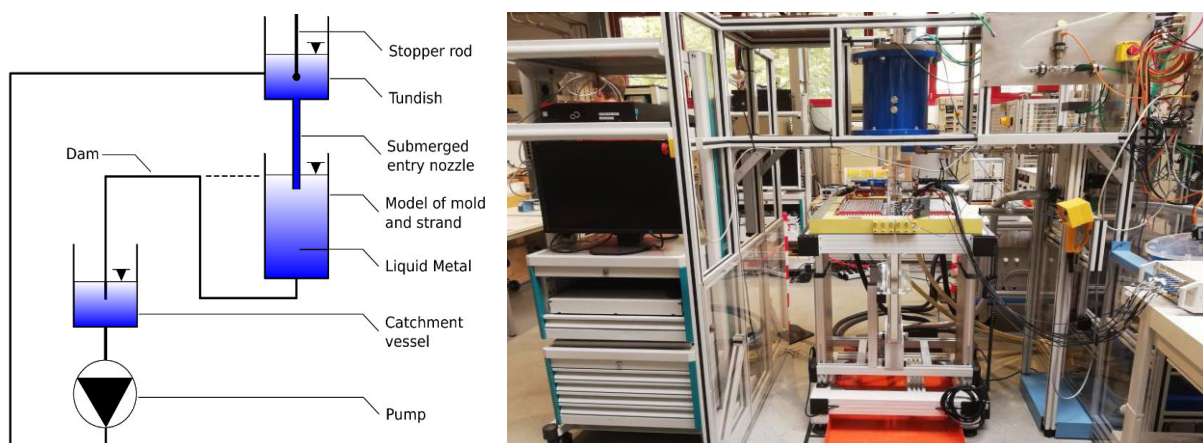


Figure 11: Mini-LIMMCAST sketch (left) and photo (right)



TOMOCON			GRANT AGREEMENT No.: 764902		
Deliverable Title: Detailed Plan for Lab Demonstrations					
Del. Rel. No.	EU Del. No.	WP No.	Lead Beneficiary	Type	Date
D5.2.	D16	WP5	TUD	Report	29.10.2019

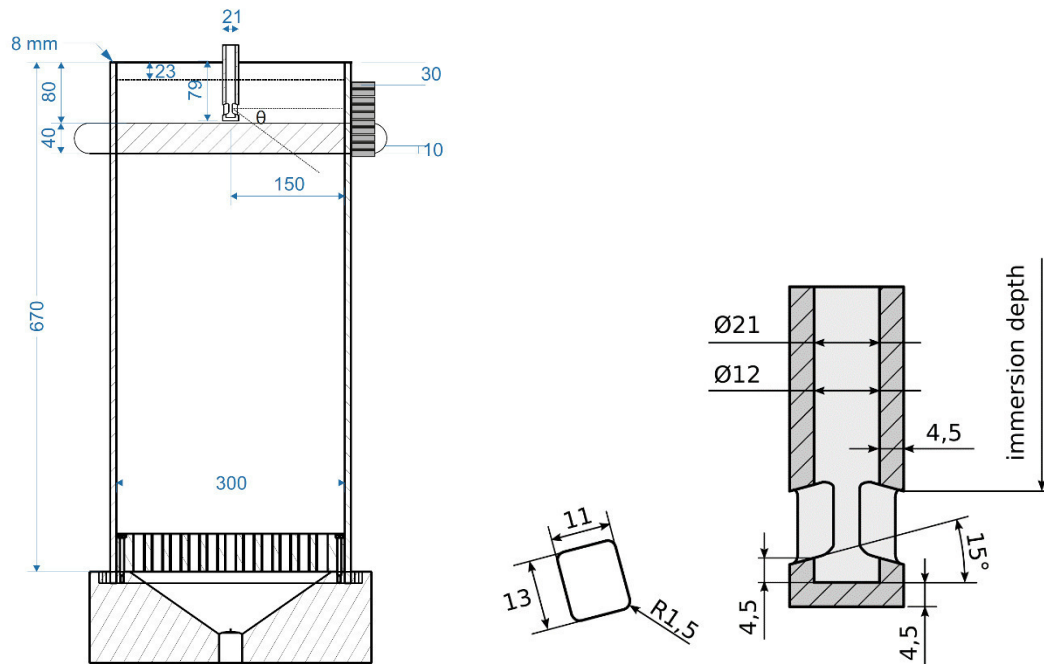


Figure 12: Dimension of the mould and SEN

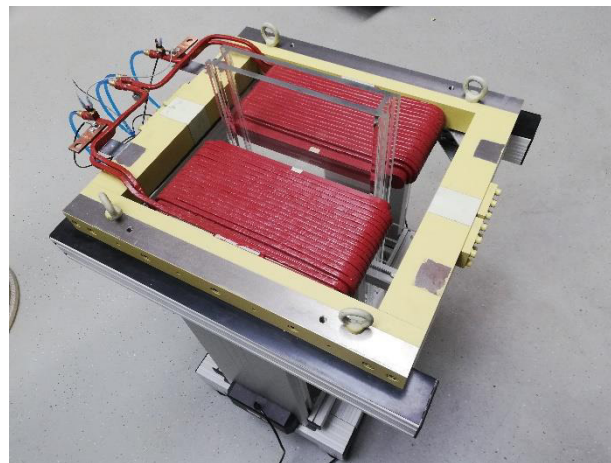


Figure 13: Electromagnetic brake (EMBr)

The stopper rod is used to adjust the flow rate through the SEN and it is actuated by pneumatics. Up to now, the opening height can only be adjusted manually. A new actuator is under development which allows for a continuous changing of the opening height. The challenge of this actuator is that a fast change as well as a precise positioning is needed.

In the industrial process, argon gas is injected into the SEN. In the demonstrator, it can be done in two ways, by injecting the gas through the tip of the stopper rod or on the side of the



TOMOCON			GRANT AGREEMENT No.: 764902		
Deliverable Title: Detailed Plan for Lab Demonstrations					
Del. Rel. No.	EU Del. No.	WP No.	Lead Beneficiary	Type	Date
D5.2.	D16	WP5	TUD	Report	29.10.2019

SEN. The gas flow rate is controlled by a MKS PR4000B gas flow / pressure controller, which can be connected to the PC by USB. A two channel controller with one valve is shown in Figure 14. Software is under development so that the gas flow controller can be operated by the control loop.

Additional actuators are in the planning stage, which will model the effects of nozzle clogging, in order to introduce defined disturbances in the system, on which the controller can react.



Figure 14: Gas flow controller (right) and power supply / remote interface

The following additional process parameters are measured: The level of the liquid metal is measured in the tundish and in the catchment tank using ultrasonic and laser distance measurement. Additionally, an ultrasonic distance measurement is used to measure the free surface level in the mould. The level in the tundish is maintained constant by adjusting the speed of the pump. This MHD pump heats up the liquid metal during the operation, thereby changing the material parameters of the liquid. In order to keep the temperature constant during a long run, the catchment tank is cooled. The temperature of the liquid metal in the catchment tank is also recorded.

3.2. Process conditions

The demonstrator will only model the fluid flow of a typical continuous casting sequence. The solidification of the liquid metal is not taken into account. A typical sequence will start with opening the stopper rod so that the liquid metal will flow into the mould, and will last one to three hours, until the stopper rod is closed. During the sequence, the EMBr will be operating and argon gas will be injected into the SEN. According to the literature, the flow structure in the mould should be stable and form a double roll. UDV measurements of the flow in the mould indicate that the flow is very stable in the actual setup over several hours. It is expected that the entire injected gas will leave the liquid metal at the free surface of the mould. The strength of the EMBr as well as the flowrate of the liquid metal and the gas will be controlled by the controller, to obtain an optimal flow condition in the mould. Special actuators



TOMOCON			GRANT AGREEMENT No.: 764902		
Deliverable Title: Detailed Plan for Lab Demonstrations					
Del. Rel. No.	EU Del. No.	WP No.	Lead Beneficiary	Type	Date
D5.2.	D16	WP5	TUD	Report	29.10.2019

will be implemented which generate a defined disturbance of the flow, on which the control loop can react.

3.3. Used experimental techniques

For this demonstrator two different tomographic sensors will be used: The actual flow in the mould will be measured by the contactless inductive flow tomography (CIFT) and the gas / liquid distribution in the SEN is detected by a combined mutual inductance and capacitance tomographic sensor. In order to validate the tomographic measurements, ultrasound Doppler velocimetry will be used, which is able to precisely measure the flow field in the mould.

3.3.1. Contactless inductive flow tomography (CIFT)

Contactless inductive flow tomography (CIFT) is a technique used for reconstructing the velocity profile in the liquid metal. It consists of two excitation coils that generate the applied magnetic field, located on the bottom and top side of the EMBr, as seen in Figure 15. They are anchored to the EMBr for robustness. On each narrow side of the mould there is an array of seven pickup coils that measure the flow induced magnetic field. The mounding of the pickup coils is made of stainless steel and anchored to the EMBr. The wires of the excitation coil are glued to the stainless steel holders which help dissipate heat and limit the distortion of the coils. Each coil has six turns in total, with an operating current between 15 A and 25 A generating a magnetic flux density between 1 mT and 2 mT in the center of the coil.

Two types of pickup coil can be used, gradiometric coils, and absolute coils. Figure 16 shows a photo of the pickup coils. Gradiometric coils measure the gradient of the horizontal magnetic field, while absolute coils measure the value of the horizontal magnetic field. The coils are connected to the AD converter. A real time data acquisition and analysis is in preparation.

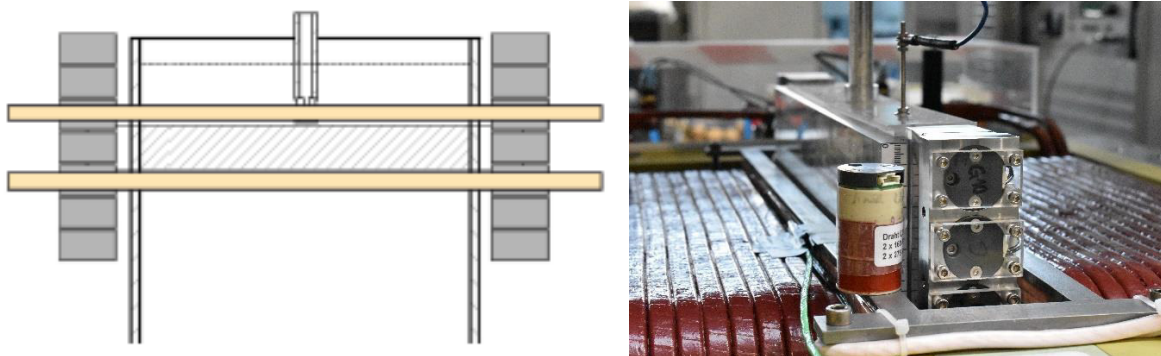


Figure 15: CIFT setup sketch (left) and photo (right)



TOMOCON			GRANT AGREEMENT No.: 764902		
Deliverable Title: Detailed Plan for Lab Demonstrations					
Del. Rel. No.	EU Del. No.	WP No.	Lead Beneficiary	Type	Date
D5.2.	D16	WP5	TUD	Report	29.10.2019



Figure 16: Gradiometric and absolute CIFT coil

3.3.2. Combined MIT and ECT

Mutual Inductance Tomography (MIT) and Electrical Capacitance Tomography (ECT) are able to reconstruct the conductivity distribution in one cross section of the SEN, thereby distinguishing between liquid metal and argon bubbles in case of a two-phase flow. MIT consists of a set of inductors (either commercial or special design) that are fitted enveloping the SEN. Each of which will be excited sequentially by a current driver; while the others act as sensors to measure the induced voltage. Hardware electronics acquire the measurement data and transmit them to the computer for image processing (background subtraction, inverse problem, etc.). Time and / or frequency difference methods will be implemented in observing the region of interest to obtain the desired information. A preliminary sensor is shown in Figure 17.

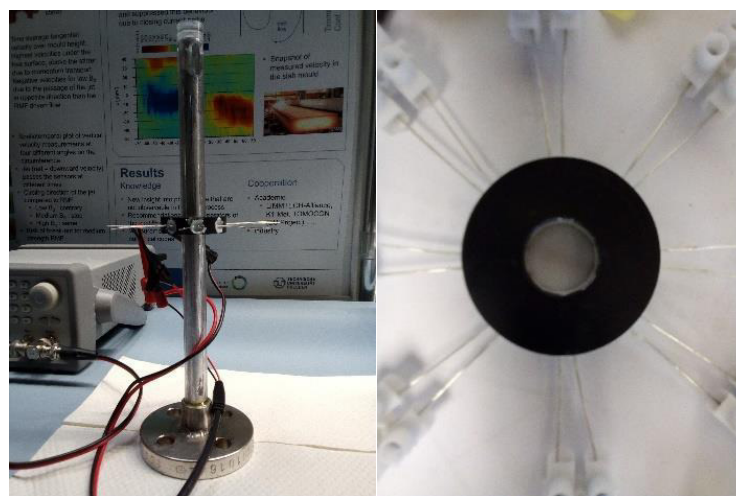


Figure 17: Preliminary MIT sensor



TOMOCON			GRANT AGREEMENT No.: 764902		
Deliverable Title: Detailed Plan for Lab Demonstrations					
Del. Rel. No.	EU Del. No.	WP No.	Lead Beneficiary	Type	Date
D5.2.	D16	WP5	TUD	Report	29.10.2019

ECT is traditionally used in industrial process monitoring such as oil / gas multi-phase flow. ECT is capable of producing a high quality image of the outer surface of the metal flow, which can be combined with MIT providing a more robust metal flow imaging. Therefore, a combined MIT / ECT sensor will be used for imaging the two-phase flow in the SEN. The MIT part will be operated with low frequencies for imaging the interior of the liquid metal and ECT will be used to detect the outer shape of the liquid metal strand.

3.3.3. Ultrasound Doppler Velocimetry (UDV)

Ultrasound Doppler velocimetry (UDV) is a well-established measurement technique that will be used to validate the results of CIFT and the MIT / ECT sensor. UDV measures the velocity component along the length of the ultrasound beam. By arranging several sensors into an array, it is possible to construct a 2D image of the velocity inside the mould. Figure 18 shows an example of the two-dimensional flow map of the horizontal velocity component in the area of the jet leaving the outlets of the nozzle.

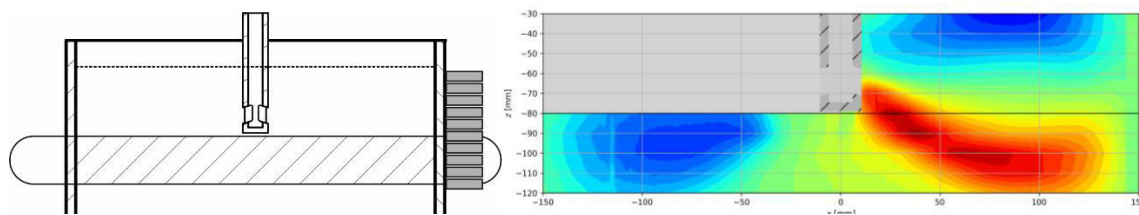


Figure 18: UDV sensor array and example of a flow map of the jet

3.4. Goals and objectives

The goals and objectives in the demonstration part of continuous casting are the design and the development of robustly working CIFT and MIT / ECT sensors. Especially, the presence of the EMBr poses large challenges to CIFT, since the effect of the ferromagnetic parts of the brake have to be taken into account. For the MIT / ECT sensor, the high velocity of the liquid metal jet in the SEN sets high demands on the temporal as well as on the spatial resolution. After the installation of the new developed sensors to the Mini-LIMMCAST facility, the flow field in the mould will be measured with a time resolution of about 1 Hz and the gas / liquid distribution has to be recorded with a frame rate of at least 100 Hz.

Since the control based on flow measurements is a complete new area of research, the control objectives have to be defined during the course of the project. In close collaboration with the industrial partners Primetals and Tata Steel, it was decided, to select the jet angle and the velocity of the free surface for control. The main quality objective is the minimization of inclusions, especially by high casting speeds. These considerations lead to the following control objectives:

- Stable double roll flow structure is preferred, while single flow or chaotic behavior has to be avoided during the process



TOMOCON				GRANT AGREEMENT No.: 764902	
Deliverable Title: Detailed Plan for Lab Demonstrations					
Del. Rel. No.	EU Del. No.	WP No.	Lead Beneficiary	Type	Date
D5.2.	D16	WP5	TUD	Report	29.10.2019

- The velocity at the free surface has to be kept in a narrow range
- The injection of argon gas should not lead to an unstable flow in the mould
- The flow structure should promote inclusions as well as single bubbles to the free surface and not in the lower part of the mould

In order to define appropriate control strategies, the effects of the brake on the flow in the single- and two-phase flow have to be investigated numerically and experimentally. Based on these data the control loop will be developed. The controller will communicate with the tomographic sensors and the actuators using TCP / IP, which is currently under development. The first results of the virtual controller indicate that the latency of TCP / IP is sufficient. Figure 19 shows a schematic of the communication structure.

As soon as Mini-LIMMCAST is equipped with all tomographic sensors and actuators, the effect of the control loop will be investigated and achieved benefits for the process will have to be evaluated. The benchmark target will be the reduction of inclusions or trapped bubbles of up to 25 % in the lower part of the mould.

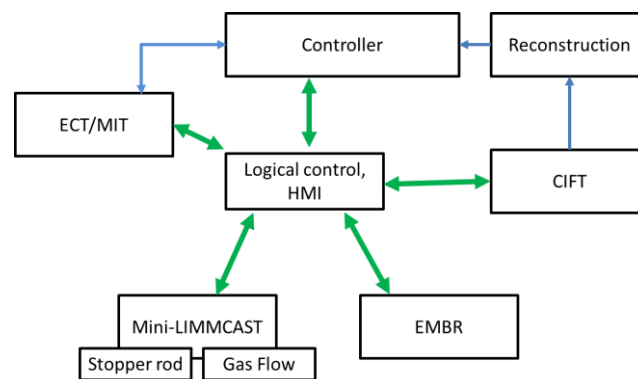


Figure 19: Communication layout



TOMOCON				GRANT AGREEMENT No.: 764902		
Deliverable Title: Detailed Plan for Lab Demonstrations						
Del. Rel. No.	EU Del. No.	WP No.	Lead Beneficiary	Type	Date	
D5.2.	D16	WP5	TUD	Report	29.10.2019	

3.5. Mode and timeline of execution

Task	responsible	2019			2020												
		M25 Sep	M26 Oct	M27 Nov	M28 Dec	M29 Jan	M30 Feb	M31 Mar	M32 Apr	M33 May	M34 Jun	M35 Jul	M36 Aug	M37 Sep	M38 Oct	M39 Nov	
Demonstrator																	
Comparison of UDV and simulation	2, 5																
Actuator for stopper rod and nozzle clogging	2																
Installation of Argon injection	2																
TCP / IP Communication framework	2																
UDV measurements for two phase flow	2, 12																
ECT / MIT test	2, 12																
Final installation of CIFT	2																
Commissioning of the control loop	2, 5, 9, 12																
CIFT																	
Real time reconstruction algorithm	2																
Compensation of the effects of the EMBR	2																
Optimization of the inverse problem	2																
Final tests of the sensor	2																
MIT / ECT																	
Development of the new sensor	12																
Investigation of real time reconstruction	12																
Final tests of the sensor	12																
Control																	
Investigation of different control methods	9																
Model development	9, 5																
Inclusion of two phase flows	9																
Implement TCP / IP communication	9, 2																
Flow simulation																	
Solver development RANS / LES / DES	5																
Single phase flow simulation with EMBr	5																
Two-phase flow simulations with EMBr	5																
Definition and test of a control scenario	5, 9, 2																



TOMOCON			GRANT AGREEMENT No.: 764902		
Deliverable Title: Detailed Plan for Lab Demonstrations					
Del. Rel. No.	EU Del. No.	WP No.	Lead Beneficiary	Type	Date
D5.2.	D16	WP5	TUD	Report	29.10.2019

4. Batch Crystallization

4.1. Facility description

Lab-scale facility

The demonstration will be implemented in the laboratory facilities of LUT at Lappeenranta, see Figure 20. The necessary analytical services for chemical analysis are available at the Analytical Center of Chemical Technology Unit (<https://www.lut.fi/web/en/cooperation-and-services/technical-services/analysis-services>). The assembly of the demonstration unit will be implemented by LUT Voima (<https://www.lut.fi/web/en/cooperation-and-services/technical-services/lut-voima>).

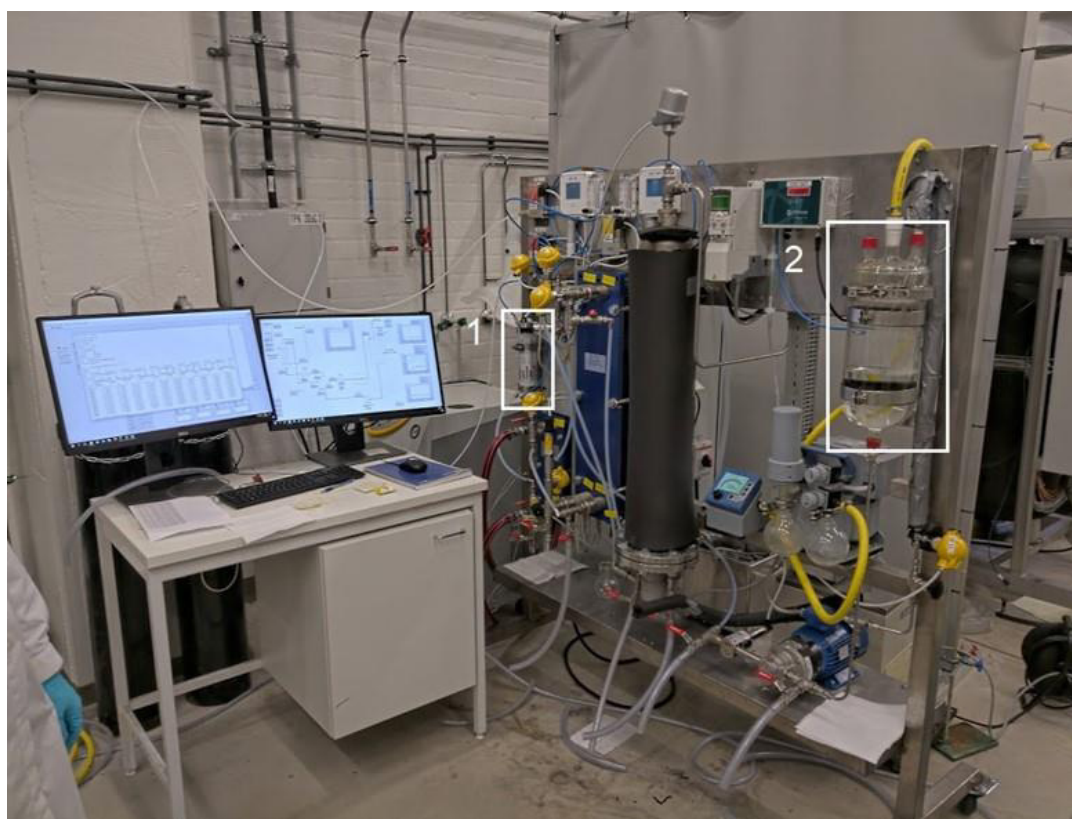


Figure 20: Intended location near the Carbon capture unit at LUT. 1 & 2: Carbon dioxide absorber & desorber

Demonstration scale description

The main part of the demonstration unit is the semi-batch crystallization of CaCO_3 using CO_2 and CaI_2 , see Figure 21. It will be combined with a carbon capture system, developed by Harri Nieminen et al. [1] as shown in Figure 22.



TOMOCON			GRANT AGREEMENT No.: 764902		
Deliverable Title: Detailed Plan for Lab Demonstrations					
Del. Rel. No.	EU Del. No.	WP No.	Lead Beneficiary	Type	Date
D5.2.	D16	WP5	TUD	Report	29.10.2019

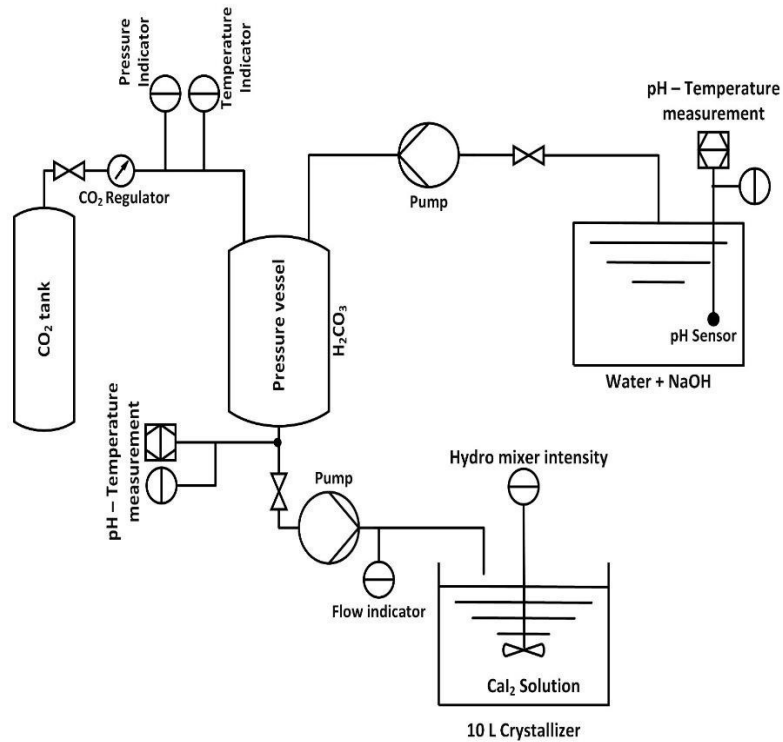


Figure 11: Calcium carbonate precipitation using CaI_2 -water solution and CO_2 dissolved in pH 12.2 water solution

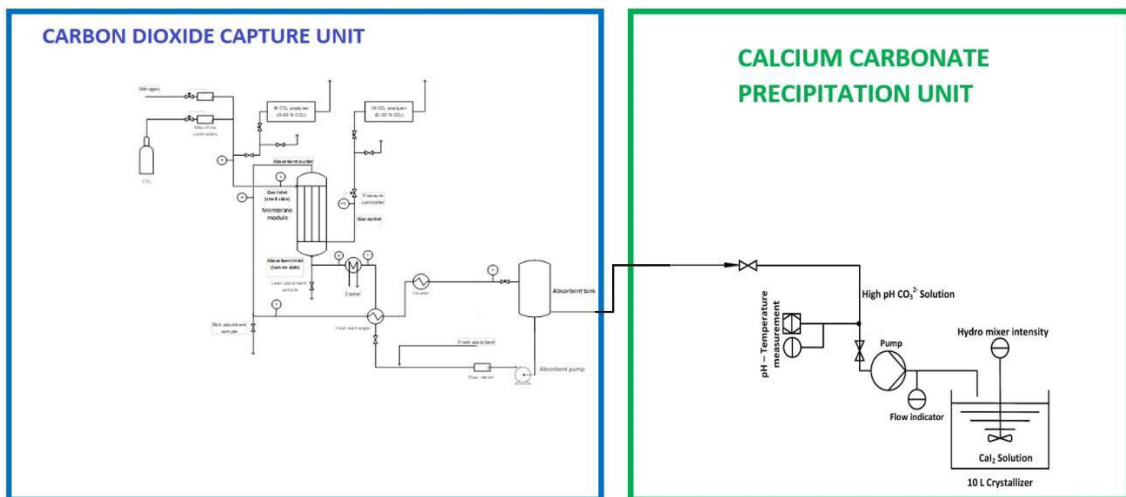


Figure 22: CaCO_3 production plant demonstration from captured CO_2

The CaCO_3 reactor size is 10 l which is operated as a fed-batch process. The carbonate (CO_3^{2-}) solution is pumped directly from a carbon dioxide capture unit to the receiving tank where the



TOMOCON				GRANT AGREEMENT No.: 764902	
Deliverable Title: Detailed Plan for Lab Demonstrations					
Del. Rel. No.	EU Del. No.	WP No.	Lead Beneficiary	Type	Date
D5.2.	D16	WP5	TUD	Report	29.10.2019

CaI₂ solution is charged. To automatically control the process, two controllable parameters are defined. The mixing intensity is controlled by using a reactor mixer, and the feed rate is controlled by using a feed pump. The 10 l reactor is equipped with electrical resistance tomography (ERT) and ultrasound tomography (UST). The tomographic sensors are assembled in a circular form around the reactor. Both UST and ERT sensors are used to measure the slurry density at different heights of the reactor. The combination of the information of the two imaging modalities is expected to provide optimal results. The sensor zone will be between 2 cm to 20 cm from the reactor bottom because of getting slurry density data in an axial direction. An additional and challenging application of ultrasound tomography is the fact of measuring the solution concentration in the reactor, which is proportional to the consumed CaI₂.

4.2. Process conditions

Chemistry and solubilities

The calcium iodide solubility in water at 20 °C is 660 g/l, and the sodium iodide (NaI) solubility is 1840 g/l. In other words, they do not crystallize during the CaCO₃ precipitation process. The calcium hydroxide solubility at 20 °C water is 1.73 g/l while the CaCO₃ solubility is 0.02 g/l which means that Ca(OH)₂ will not precipitate when feeding the NaOH – CO₂ solution into CaI₂ water. The solubility data for CO₂ (Figure 23) and CaCO₃ (Figure 24) are introduced.

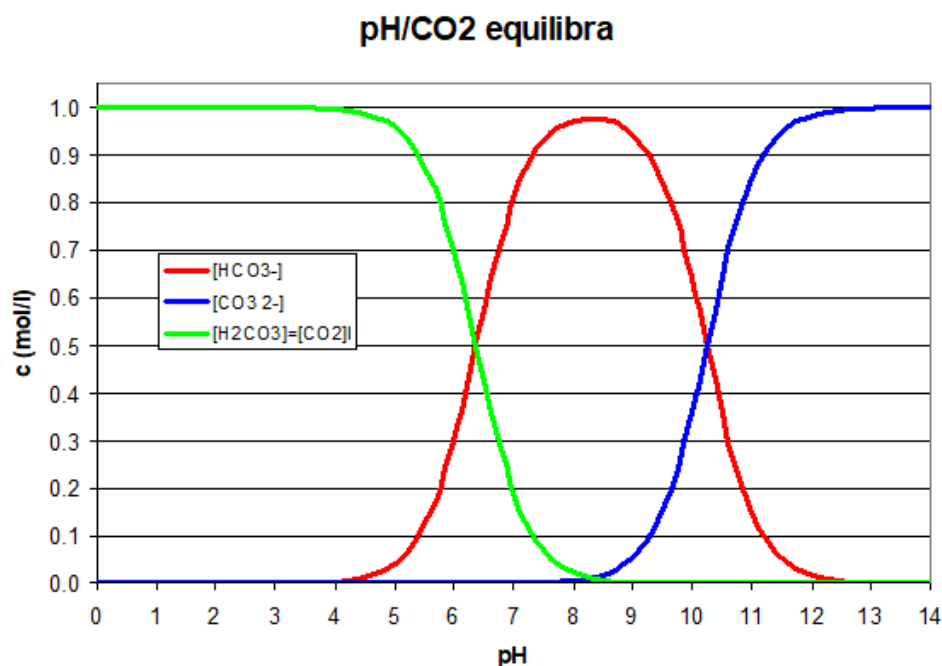


Figure 23: CO₂ solubility at 25 °C as a function of pH



TOMOCON			GRANT AGREEMENT No.: 764902		
Deliverable Title: Detailed Plan for Lab Demonstrations					
Del. Rel. No.	EU Del. No.	WP No.	Lead Beneficiary	Type	Date
D5.2.	D16	WP5	TUD	Report	29.10.2019

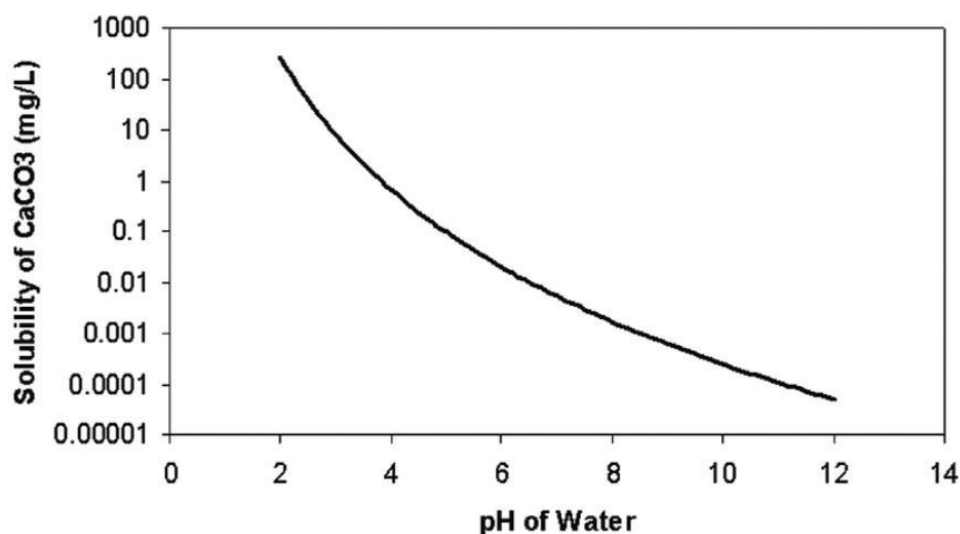


Figure 24: CaCO₃ solubility at 25 °C in pH range 2-12

Process window for experiments

The semibatch crystallization process of calcium carbonate (CaCO₃) is carried out based on the following chemical equation,



As shown in the reaction equation 1, the crystallization occurs by the addition of different concentrations of high-pH carbonate ions (CO₃²⁻) to the calcium iodide (CaI₂)-water solution. Certain carbonate concentrations are achieved by controlling the pH of water for the CO₂ dissolution. The higher boundary of the process window considered in this work is the saturation point of the CO₂ dissolution in water at ambient temperature and pressure, which is 1 mol/lit at pH 12.2.

During the crystallization process, the concentration of NaI varies between 0-1 mol/l, the CaCO₃ slurry density variation would be between 0-2 vol-%, the CaI₂ concentration between 1-0 mol/l.

4.3. Used experimental techniques

Crystallization techniques

The system of interest is the reaction type crystallization for the semibatch precipitation process of calcium carbonate (CaCO₃) in a highly alkaline solution at atmospheric pressure (1 atm) and ambient temperature (21 ± 2 °C). Small-scale lab experiments were carried out at several operating conditions and the effects of the variation of the agitation rate, feed flow rate and feed concentration on the particle size were investigated.



TOMOCON			GRANT AGREEMENT No.: 764902		
Deliverable Title: Detailed Plan for Lab Demonstrations					
Del. Rel. No.	EU Del. No.	WP No.	Lead Beneficiary	Type	Date
D5.2.	D16	WP5	TUD	Report	29.10.2019

Analytics

The particle size distribution (PSD) of the final product from each semibatch operation is measured by the laser diffraction method in a particle size analyzer Mastersizer 3000 (Malvern Instruments, UK). The crystal lattice analysis through X-ray diffraction is done with a Bruker D8 Advance X-ray diffractometer and for obtaining the surface structures of the solid samples, a scanning electron microscope (SEM) SU 3500 Hitachi SEM is used. Additionally, to ensure the composition of the solids, an energy-dispersive X-ray spectroscopy (EDS) of some of the selected samples was obtained by the SEM device. Dynamic pH measurements are determined using a Consort pH meter with a Consort pH electrode.

It is expected to utilize an electrical resistance tomography (ERT) device for evaluating the differences in the solid density inside the reactor during the crystallization process. The denser regions within the reactor would have a different conductivity as compared to the regions with lesser density. Along with this, the suspension height would be measured vertically. The solid suspension height could be proportional to the average particle size through settling velocity, suspension density or final yield.

Moreover, it is also expected that an ultrasound computed tomography (USCT) system will be employed for conducting imaging based on the transmission ultrasound tomography method. USCT will focus on characterizing the process by monitoring the density changes of the slurry.

4.4. Goals and objectives

Set-up conditions to control semibatch crystallization

Based on the laboratory observations, a series of reasonable assumptions have been made for the current system. Since the precipitation is reactive crystallization, its kinetics are not related to macroscale times; so, it is scale independent. Additionally, the CaCO_3 precipitation reaction within the reactor is considered as instantaneous.

The proposed process is greatly affected by the mixing intensity (mesomixing) and the feed flow rate. The mixing at the meso-scale is responsible for the concentration distribution and the spreading of solid particles in the crystallizer. The feed rate of the reagent to the receiving tank also plays a significant role on the particle diameter and its quality. One of these variables could be used in a control loop to regulate the semibatch crystallization process.

For this purpose, the design of experiments software (e.g., MODDE Pro by Umetrics) provides a framework to conduct a sensitivity analysis of the output parameter (mean diameter) to the process input variables (mixing rate, feed rate). This makes it possible to select one parameter that greatly affects the output.

The output signal of the tomographic measurement will be correlated with the mean particles size through the hindered settling velocity. The settling velocity could be obtained by knowing the distance between the sensor layers and time of the measurements, which provides information about the average diameter of the particles. The feed rate (or mixing intensity) could be controlled accordingly to provide particles with specific sizes.



TOMOCON				GRANT AGREEMENT No.: 764902			
Deliverable Title: Detailed Plan for Lab Demonstrations							
Del. Rel. No.	EU Del. No.	WP No.	Lead Beneficiary	Type	Date		
D5.2.	D16	WP5	TUD	Report	29.10.2019		

4.5. Mode and timeline of execution

TOMOCON Batch Crystallization Group: Estimated Timetable and Workplan

#	Task	Project Months	25	26	27	28	29	30	31	32	33	34	35	36	37	38	39	40
			9	10	11	12	1	2	3	4	5	6	7	8	9	10	11	12
			2019	2019	2019	2019	2020	2020	2020	2020	2020	2020	2020	2020	2020	2020	2020	2020
	ESR																	
1	Small-scale crystallization experiments	8	<input checked="" type="checkbox"/>															
2	TOMOCON virtual demo results	8		<input checked="" type="checkbox"/>														
3	IFAC 2020 manuscript	8			<input type="checkbox"/>													
4	Manuscript of small-scale crystallization experiments	8, 11, 13			<input type="checkbox"/>	<input type="checkbox"/>												
5	Final numerical simulations of the experiments (small scale) (FLUENT)	8				<input type="checkbox"/>	<input type="checkbox"/>	<input type="checkbox"/>	<input type="checkbox"/>									
6	Demo unit planning & build-up	8			<input type="checkbox"/>													
7	Crystallization scale-up numerical simulation (FLUENT)	8								<input type="checkbox"/>	<input type="checkbox"/>							
8	CONTROL; learning / improvement / development (Possible image processing & fuzzy control approach?) (+Secondment @ULIB)	8						<input type="checkbox"/>		<input type="checkbox"/>								
9	Demo-scale experiments	8								<input type="checkbox"/>	<input type="checkbox"/>							
10	Possible experiments with PixAct device	8									<input type="checkbox"/>							
11	Possible manuscript with PixAct	8										<input type="checkbox"/>						
12	Improvements & building up the ERT sensors + algorithms	11			<input type="checkbox"/>		<input type="checkbox"/>											
13	Improvements & building up the UST sensors + algorithms	13			<input type="checkbox"/>		<input type="checkbox"/>											
14	LUT Summer School	TOMOCON											<input type="checkbox"/>					
15	ERT Installation + Experiments	8, 11														<input type="checkbox"/>	<input type="checkbox"/>	
16	UST Installation + Experiments	8, 13													<input type="checkbox"/>	<input type="checkbox"/>	<input type="checkbox"/>	
17	TOMOCON lab demo results	8, 11, 13															<input type="checkbox"/>	
18	Manuscript of the crystallization with ERT	8, 11, 13																<input type="checkbox"/>
19	Manuscript of the crystallization with UST	8, 11, 13																<input type="checkbox"/>
20	TOMOCON Textbook (M42)	8, 11, 13																<input type="checkbox"/>



TOMOCON			GRANT AGREEMENT No.: 764902		
Deliverable Title: Detailed Plan for Lab Demonstrations					
Del. Rel. No.	EU Del. No.	WP No.	Lead Beneficiary	Type	Date
D5.2.	D16	WP5	TUD	Report	29.10.2019

4.6. References

- [1] H. Nieminen, L. Järvinen, V. Ruuskanen, A. Laari, T. Koiranen, J. Ahola, Insights into a membrane contactor based demonstration unit for CO₂ capture, Sep. Purif. Technol. (2019). doi:10.1016/j.seppur.2019.115951.

